Electronic Supplementary Material (ESI) for RSC Advances.

Electronic Supplementary Information (ESI)

Influence of normal load on the three-body abrasion behaviour of monocrystalline silicon with ellipsoidal particle

Junqin Shi, Juan Chen, Xinqi Wei, Liang Fang, Kun Sun, Jiapeng Sun, Jing Han

1. Simulated results of shear velocity 5 m/s

It is well known that the 50 ms^{-1} velocity of the upper specimen is much higher than the experimentally relevant velocities. In order to make the simulated results be closer to the results in experiments, some simulations were performed additionally under the upper specimen velocity of 5 ms^{-1}. Fig. 5 shows the atomic instantaneous configurations at normal load of 120 nN and 200 nN. In Fig 5(a), the particle shows an unceasing rolling movement in the whole simulation process although its rotation is very slow. Contrarily, the particle remains sliding after an initial rolling as the normal load is 200 nN in Fig. 5(b), similar to the sliding movement in Fig. 2(d) and (e). In Fig. S1, the displacement of the upper specimen increases continuously at normal load 120 nN, but it only shows a slight fluctuation at normal load 200 nN. In Fig. S2, the angular velocity of ellipsoidal particle fluctuates above zero at normal load 120 nN, while it fluctuates around zero at normal load 200nN. All the results indicate that the movement trend of ellipsoidal particle is not changed due to the decrease of shear velocity.

Furthermore, for the 5 ms^{-1} velocity of upper specimen, although the movement pattern of ellipsoidal particle changes from rolling to sliding as the normal load increases from 120 nN to 200 nN, the force evolution shows the same trend. Namely, the friction force increases from zero and then remains constant while the normal force remains constant with the increase of time, as shown in Fig. S3 (ESI†). This, different from the cases under high velocity in Fig. 9, is because that the low velocity leads to a steadier movement of particle.

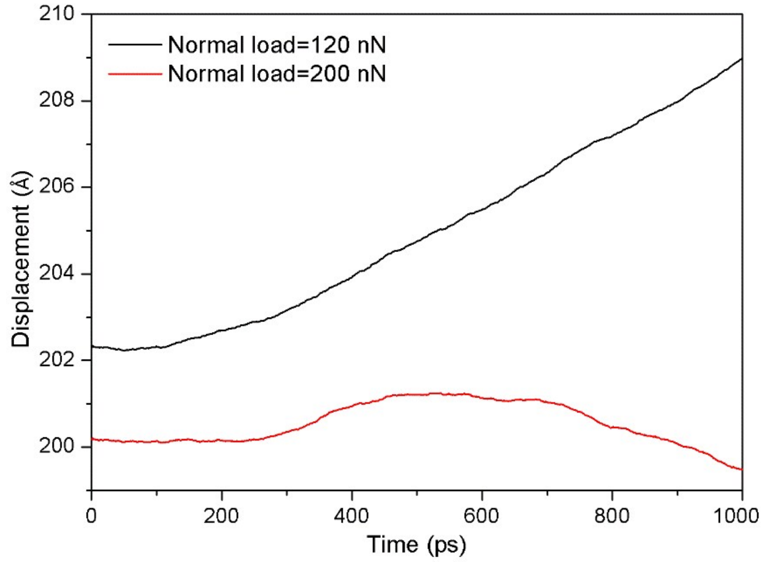

Fig. S1 Displacement of the upper specimen along *y*-[010] direction vs. time.

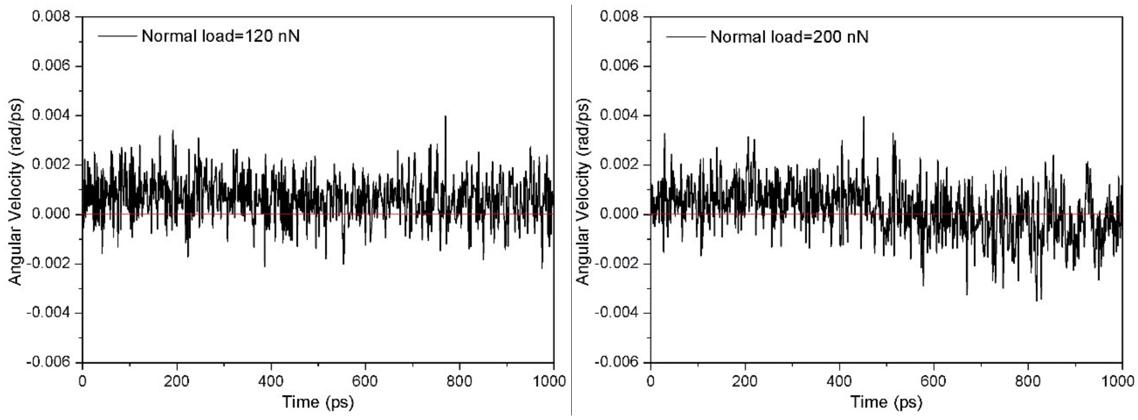

(a) (b)

Fig. S2 Angular velocity of abrasive centre-of-mass vs. time at normal load (a) 120 nN and (b) 200 nN.

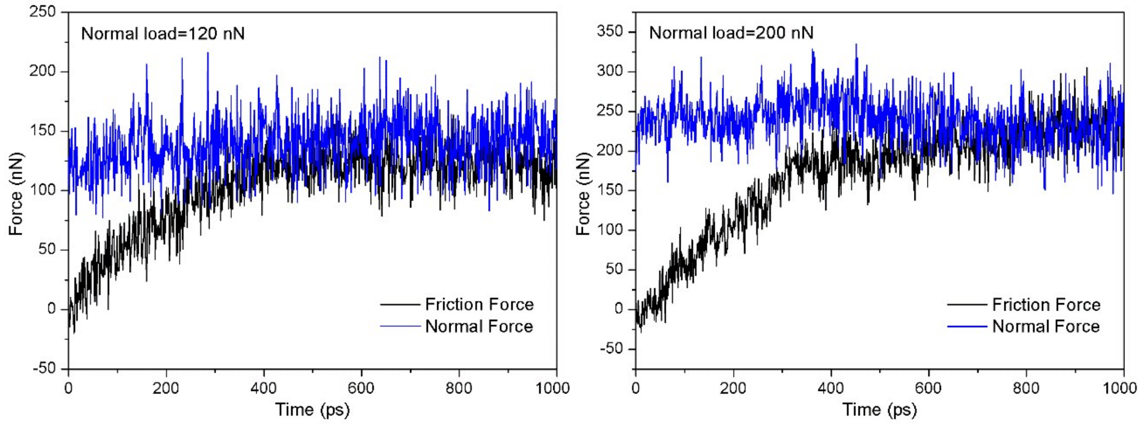

(a) (b)

Fig. S3 Friction force and normal force vs. time at normal load (a) 120 nN and (b) 200 nN.

2. Calculation method of *e*/*h* value

In the manuscript, Fig. 6 depicts the force between the moving ellipsoidal particle and the bottom silicon specimen. The interaction between particle and the upper specimen is omitted due to the system symmetry. Point *S* is assumed as a central contact point of distributed forces on the particle surface, and point *O*, the centroid of the ellipsoidal particle. This simplified model has been reported by the present authors. *N* and *F* are normal load and friction force acting on the particle by the surface of specimen, and *v* represents the movement direction of upper specimen.

From the previous work by the present authors, as shown in Fig. S4 for a spherical particle where there is

$$e=\frac{4}{3\pi}\left(r_1+r_2\right) \tag{1}$$

$$h=\frac{2}{3}\left(\frac{r_1\sin^3\alpha_1}{\alpha_1-\sin\alpha_1\cos\alpha_1}+\frac{r_2\sin^3\alpha_2}{\alpha_2-\sin\alpha_2\cos\alpha_2}\right) \tag{2}$$

$$e/h=\frac{2P}{\pi^2R^2H_1}\cdot\frac{\xi_1^{1/2}+\xi_2^{1/2}}{\xi_1^{3/2}+\left(H_2/H_1\right)\xi_2^{3/2}},$$

$$\xi_1=\left[1-\left(1-\frac{P}{\pi R^2H_1}\right)^2\right],\ \xi_2=\left[1-\left(1-\frac{P}{\pi R^2H_2}\right)^2\right] \tag{3}$$

where *P* is the normal load, *R* is the particle size, H_1 and H_2 are the surface hardness of the upper and bottom specimens.

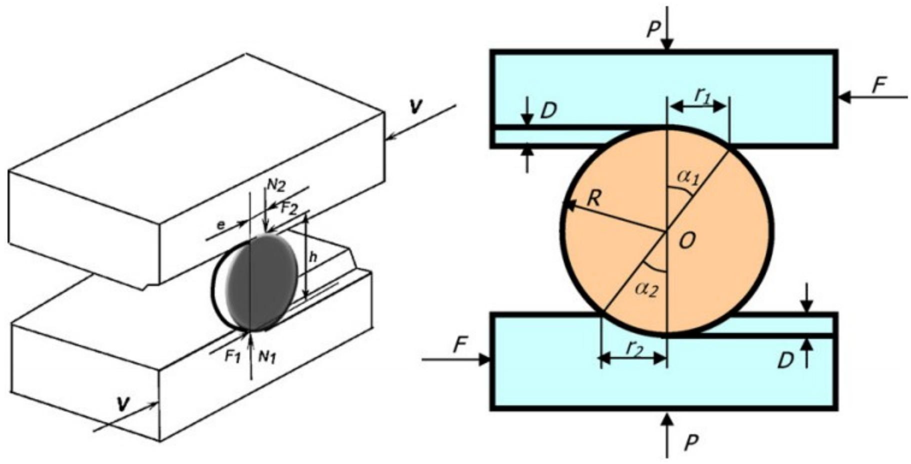

Fig. S4 Schematic illustration of force analysis on an abrasive particle.

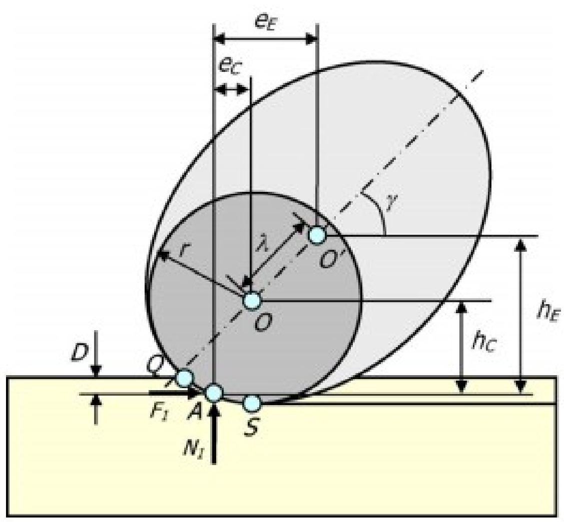

Fig. S5 Parameters of ellipsoidal abrasive particle cross-section using a spherical approximation method.

To illustrate the ellipsoidal particle movement pattern, a circle approximation approach is used to get indentation and contact point position as shown in Fig. S5. For simplicity, an equivalent circle approach is used in which two-dimensional analysis is applied. A circle and an ellipsoid are overlapped together to make the circle particle boundary coincident with the ellipsoid at the geometric lowest point *S* and the contact point of the circle *Q* with surface also coincident with that of the ellipsoid as shown in Fig. S5. In Fig. S5, a separated angle is defined as rotation angle of ellipsoid γ between the center of a circle point *O* and the center of ellipsoid *O'*. *A* becomes a working point of resultant force N_1 and F_1 for the circle. *r* is the radius of the circle and λ is the center distance of the circle and ellipsoid. Thus, the resultant forces, i.e. N_1 and F_1 of the circle can be approximately considered equal to that of the ellipsoid.

Because e/h value for the equivalent circle can be easily got from expressions (1)-(3), the e/h for the ellipsoid can be directly got by following equations, where e_E is a horizontal distance of the ellipsoid centroid, e_C a horizontal distance of the circle centroid, h_E a vertical distance of the ellipsoid centroid and h_C a vertical distance of the circle centroid.

$$\begin{cases} e_E = e_C + \lambda \cos\gamma \\ h_E = h_C + \lambda \sin\gamma \end{cases} \tag{4}$$